RSC Advances

PAPER

View Article Online
View Journal | View Issue



Cite this: *RSC Adv.*, 2023, **13**, 15881

# High-efficiency removal of tetracycline from water by electrolysis-assisted NZVI: mechanism of electron transfer and redox of iron

Xiangyu Wang, *[a] Xiangmei Wang,[a] Iseult Lynch[b] and Jun Ma[c]

A low-cost, stable and non-precious metal catalyst for efficient degradation of tetracycline (TC), one of the most widely used antibiotics, has been developed. We report the facile fabrication of an electrolysis-assisted nano zerovalent iron system (E-NZVI) that achieved TC removal efficiency of 97.3% with the initial concentration of 30 mg $L^{-1}$ at an applied voltage of 4 V, which was 6.3 times higher than the NZVI system without an applied voltage. The improvement caused by electrolysis was mainly attributed to the stimulation of corrosion of NZVI, which accelerated the release of $Fe^{2+}$. And $Fe^{3+}$ in the E-NZVI system could receive electrons to reduce to $Fe^{2+}$, which facilitated the conversion of ineffective ions to effective ions with reducing ability. Moreover, electrolysis assisted to expand the pH range of the E-NZVI system for TC removal. The uniformly dispersed NZVI in the electrolyte facilitated the collection and secondary contamination could be prevented with the easy recycling and regeneration of the spent catalyst. In addition, scavenger experiments revealed that the reducing ability of NZVI was accelerated in the presence of electrolysis, rather than oxidation. TEM-EDS mapping, XRD and XPS analyses indicated that electrolytic effects could also delay the passivation of NZVI after a long run. This is mainly due to the increased electromigration, implying that the corrosion products of iron (iron hydroxides and oxides) are not formed mainly near or on the surface of NZVI. The electrolysis-assisted NZVI shows excellent removal efficiency of TC and is a potential water treatment method for the degradation of antibiotic contaminants.

Received 12th February 2023
Accepted 11th April 2023

DOI: 10.1039/d3ra00954h

rsc.li/rsc-advances



## 1. Introduction

With the development of modern science and technology, the water environment is subject to more and more exogenous pollution, such as industrial wastewater, organic chemical materials and antibiotic wastewater produced by drug abuse.[1] However, antibiotics are difficult to degrade completely, and antibiotic resistance can develop when antibiotics in the water environment enter animals and humans.[2] Antibiotic resistance constitutes a world-wide serious issue for public health safety.[3,4] Tetracycline (TC), one of the most commonly used antibiotics, can be used to treat infectious diseases in humans, and as an additive to animal drugs in aquaculture.[5] However, most TCs are discharged into the environment in the form of their original states or intermediate degradation products, which poses a potential risk to aquatic organisms and the environment due to their poor biodegradability.[6,7] Therefore, there is an urgent need for an effective remediation technique because of the consumption, excretion, and persistence of TC. Great efforts have been made for TC removal, including adsorption,[8,9] co-precipitation,[10] membrane separation,[11] photocatalysis,[12] electrocatalysis,[13] photoelectrocatalysis[14] and biological treatment.[15] Nano zero-valent iron (NZVI) is one of the most powerful reducing agents due to its high reactivity, large specific surface area and low fabrication cost.[16] NZVI is not only a direct electron donor but also a source of $Fe^{2+}$,[17] and it is expected to be used in wastewater treatment.[18] The spontaneous corrosiveness of the NZVI surface results in the formation of $Fe^{2+}$ and $Fe^{3+}$, and the removal of pollutants by NZVI is mainly achieved by adsorption and reduction on its surface.[19] However, NZVI suffers from some limitations such as low reusability, self-oxidation, and instability.[20] Previous studies on the modification of NZVI often focused on improving its reducibility or enhancing the performance of NZVI through pre-corrosion strategies such as the presence of coexisting cations ($Mg^{2+}$, $Co^{2+}$).[21] Few studies have been conducted to improve the reusability of NZVI by simultaneously promoting the corrosion of $Fe^0$ to release more $Fe^{2+}$ to accelerate the removal of contaminants while keeping it from being passivated and thus losing its reduction activity.

Electrochemical techniques have been applied to the degradation of pollutants and to overcome the uncontrollable reactivity of NZVI. In the previous study, nanocomposites were

[a]*Faculty of Environmental Science and Engineering, Kunming University of Science and Technology, Kunming 650500, China. E-mail: imusthlee2014@sina.com*
[b]*School of Geography, Earth and Environmental Sciences, University of Birmingham, Birmingham B15 2TT, UK*
[c]*School of Municipal and Environmental Engineering, Harbin Institute of Technology, Harbin 150090, China*

prepared by immobilizing NZVI nanoparticles in millimeter-scale porous hollow graphite columns using polymeric microbeads as carriers and columnar electrochemical reactors were constructed as molded flow reactors for the selective degradation of nitrate.[22] Metal-free electrodes NZVI/ACF with different iron loadings were also prepared by the conventional impregnation method and their electrocatalytic bromine reduction performance was investigated in a two-chamber electrochemical reactor.[20] The application of weak magnetic fields (WMF) or pre-magnetization can promote the corrosion of $Fe^0$ and accelerate the removal of heavy metals and organic contaminants.[23–26] The improvement of contaminants removal from $Fe^0$ induced by WMF may be mainly attributed to the Lorentz force, while the magnetic field gradient force can stimulate the continuous corrosion of $Fe^0$.[27] It is clear that the corrosion of $Fe^0$ determines the removal of contaminants. Therefore, methods that can promote $Fe^0$ corrosion to release more ferrous ions are beneficial for the contaminants removal. Recently, studies have shown weak magnetic fields promote the corrosion of $Fe^0$ and the mechanism of electrochemically assisted oxidation processes using petiolate and NZVI. At current densities ranging from 0 to 5 mA $cm^{-2}$, NZVI particles were completely converted to iron (hydroxide) oxides such as hydrous iron ore, and magnetite. At low current densities, NZVI particles were completely converted to iron oxides, such as ferric hydroxide, lepidolite and magnetite. At high current densities, $Fe^0$ was converted to a small amount of $Fe^{2+}$ and it facilitated the retention of $Fe^0$ phase.[28] Most previous reports on electrically assisted NZVI have focused on the oxidation of NZVI, which was used as a feedstock to make electrodes. When NZVI was modified as a $Fe^{2+}$ donor for the electrode material, due to the high activity of NZVI, it tended to break off from the electrode during the reaction, which shortened the service life of the electrode and also negatively affected the pollutant removal effect. Therefore, from the viewpoint of reducing the loss of electrode materials during the reaction and improving the efficiency of pollutant removal, adding NZVI directly into the electrolyte solution and promoting the release of $Fe^{2+}$ from NZVI by the electrolysis-assisted method was more convenient and faster in terms of pollutant treatment.

In view of this, the main objective of our study was to develop an efficient electrolysis-assisted NZVI (E-NZVI) system. For the first time, our study investigated the effect of electrolysis-assisted NZVI on TC removal based on accelerated oxidation and reduction mechanisms. The secondary objectives included: (1) to investigate the effect of key operating parameters on the promotion efficiency of NZVI in the presence of electrolysis (E-NZVI), (2) to systematically characterize the structure and composition of corrosion products during TC removal by pristine NZVI (pri-NZVI) and E-NZVI, and (3) to elucidate the mechanism of TC removal by the E-NZVI system.

# 2. Materials and methods

## 2.1 Materials

Potassium borohydride ($KBH_4$), ferrous sulfate heptahydrate ($Fe_2SO_4 \cdot 7H_2O$), potassium chloride (KCl), sodium sulfate ($Na_2SO_4$), tetracycline, anhydrous ethanol, hydrochloric acid (HCl), sodium hydroxide (NaOH), methanol (METH) and dimethyl sulfoxide (DMSO) were purchased from Sinopharm Chemical Reagent Co. Ltd Shanghai, China. All chemicals are chemical analytical grade. Deionized water (18.2 MΩ cm, 25 °C) was produced using the MILI-Q reference ultrapure laboratory water system (Merck Microporous, USA). All glassware and reactors were soaked in $HNO_3$ overnight and rinsed with ultrapure water prior to use. Graphite electrode rods used for the experiments were purchased from the Haitian Muzi Graphite Manufacturing Plant, Tianjin, China.

## 2.2 Experiments

**2.2.1 Electrochemical reaction system.** The electrodes were placed in parallel in a polypropylene cube electrolytic reactor (140 × 50 × 180 $mm^3$). A platinum electrode (100 × 100 × 1 $mm^3$) was used as the anode and a graphite rod as the cathode (the volume of the part immersed in the electrolyte is 200π $mm^3$), and the distance between the anode and the cathode is 40 mm. The electrochemical workstation is a Shanghai C&H chi660E and the operating voltage is monitored accordingly.

**2.2.2 Batch test and condition optimization.** The performance and mechanism of the E-NZVI system were investigated *via* batch experiments by using TC as the target contaminant. The reaction vessel was a cylindrical (7 cm in diameter and 10 cm in height) glass electrochemical cell with Teflon. A stock solution of 30 mg $L^{-1}$ of TC (target contaminant) and 100 mM sodium sulfate (as electrolyte) was prepared and added to the electrolytic cell at a volume ratio of 1 : 1 during the reaction. For analysis, the solution was sampled every 30 min and the absorbance of the solution was tested by UV spectrum spectrophotometer.

To obtain the optimal reaction conditions, the initial pH value was manually adjusted by dropwise addition of either 0.5 M NaOH or 0.5 M HCl. To investigate the effect of different NZVI dosages on the removal of TC in the E-NZVI system, different amounts of NZVI particles were added to the electrolyte before the reaction. Batch experiments were conducted into the solution containing 30 mg L per TC at NZVI dosing levels of 0–60 mg $L^{-1}$. For investigation of the effect of different applied voltages on the performance of E-NZVI, batch experiments were conducted by adding NZVI (30 mg $L^{-1}$) to the E-NZVI system containing 30 mg per L TC at applied voltages of 0, 1.0, 2.0, 3.0, and 4.0, 4.5 V, by marking systems as E-NZVI@0.0V, E-NZVI@1.0V E-NZVI@2.0V, E-NZVI@3.0V, E-NZVI@4.0V, and E-NZVI@4.5V, respectively.

An equivalent amount of about 4 mL was taken at a predetermined reaction time (0–150 min) and the sample was immediately filtered through a 0.45 μm membrane. A filtered sample of 1 mL was taken and diluted to 10 mL and kept at 22 ± 0.5 °C for further analysis. Finally, the wasted NZVI (reacted with TC solution after 150 min) was collected by filtration, rinsed with deionized water, and dried for further characterization.

**2.2.3 Analysis and characterization.** The morphology of the structural solid phase was obtained using an FEI-TF20, an

 

energy spectrum model super-X transmission electron microscope and an energy dispersive spectrometer (EDS; Oxford Instruments, UK). The morphology of the aged NZVI solid products was further investigated. Surface sensitive analysis was performed with an X-ray photo-electron spectrometer (Thermo Fisher Scientific K-Alpha) under the X-ray source: monochromatic Al-Kα source, energy: 1486.6 eV, filament power: 72 W.

# 3 Results and discussion

## 3.1 Comparison of activities of pristine iron, electric-only, and electric-assisted iron on tetracycline

In order to quantitatively characterize the reactivity of NZVI with or without electrolysis, the removal efficiencies of TC under different conditions of pristine iron (pri-NZVI), electricity only and electrically assisted iron (E-NZVI) were compared. As shown in Fig. 2a, the removal efficiency of TC after 150 min was in the order of E-NZVI > Electrolysis > pri-NZVI. TC removal efficiency with pristine NZVI was only 15.46%. The removal mechanism of contaminants with pristine NZVI is mainly through the corrosion effect of NZVI, the production of $Fe^{2+}$, the consumption of $H^+$ by NZVI under acidic conditions, and ultimately the increase in solution pH.[29] It has been reported that hydrogenation reduction reactions are the main mechanism for antibiotic removal by NZVI and that reactive substances such as H produced during the redox process of NZVI induce the reduction of TC by NZVI.[7] Although NZVI has high reduction activity, pristine NZVI alone is inefficient in TC removal due to decreased activity caused by aggregation and self-oxidation.

For a raw electrolytic process, when applied voltages = 4 V; $C_0$ = 30 mg $L^{-1}$; pH = 7.11; $t$ = 298 K, the removal efficiency of TC by electrocatalysis is only 64.32% in 150 min through the direct electrochemical oxidation and indirect electrochemical oxidation of the electro-generated oxidant.[28] In contrast, E-NZVI achieved a removal efficiency of 96.18% for TC, much higher than that of the pristine NZVI and raw electricity process. The excellent TC removal performance of E-NZVI might be explained by the acceleration in the corrosion rate of NZVI with electrolysis in the E-NZVI system that promotes the release of $Fe^{2+}$. This is attributed to the release of electrons from the anode in the presence of the applied voltage, resulting in an electron-deficient oxidizing atmosphere that will form near the anode, thus allowing the accelerated oxidation of NZVI and its faster release of $Fe^{2+}$, thus accelerating the removal of TC. Meanwhile, $Fe^{3+}$ generated with corrosion were converted into $Fe^{2+}$. This transformation is attributed to the cathode gaining electrons due to the applied voltage in the E-NZVI system, which causes a reducing environment to form near the cathode, where $Fe^{3+}$ near the cathode gets electrons to reduce to $Fe^{2+}$.[30]

## 3.2 TEM-EDS analysis

TEM-EDS images of reacted NZVI in Fig. 1a after the reaction without electrolysis assistance and Fig. 1b after the reaction at 4 V in the E-NZVI system further revealed the oxidation of NZVI after the reaction. The high-magnification images clearly show that each NZVI particle consists of a dense nucleus with a thin shell wrapped around the nucleus. There is a significant difference between the morphologies of the reacted NZVI with and without electrolytic assistance. The oxide on the surface of NZVI without electrolytic assistance is much thicker than that with electrolytic assistance. As shown in TEM-based EDS elemental mappings in Fig. 1, the color distributions of Fe (Kα)

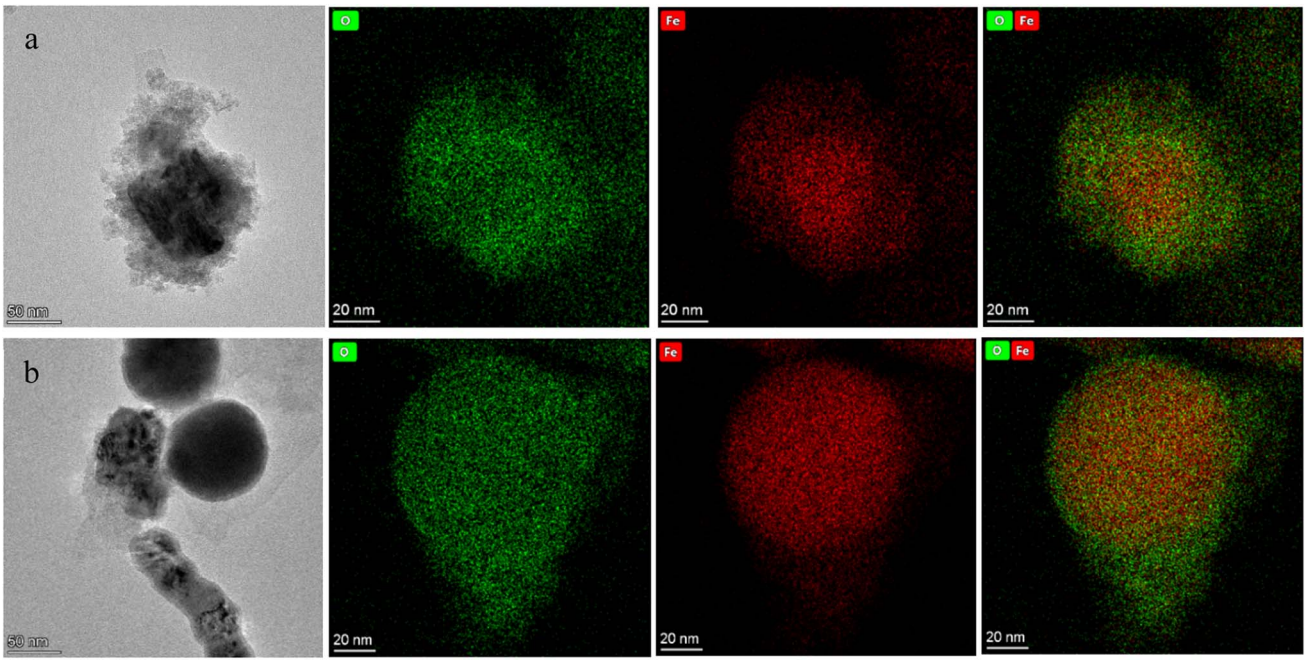


Fig. 1 TEM-EDS mappings of iron (Fe), oxygen (O), and image of spent NZVI: signals were collected from the NZVI after a 150 min reaction with 30 mg $L^{-1}$ of TC under (a) without electrolysis assist; (b) with electrolysis assist.

and O (Kα) elements on the NZVI surface demonstrate that the NZVI shell layer is dominated by Fe, O and the ratio of Fe to O on NZVI particles without electrolytic assistance is dramatically reduced, indicating that NZVI is severely oxidized without electrolytic assistance, and this process can be greatly improved by electrolytic assistance. This is because NZVI corrodes rapidly in contact with water and oxygen under conditions without electrolytic assistance, and cannot be recovered, while in the E-NZVI system, due to the presence of electrodes, the electron movement in the system will both accelerate $Fe^0$ corrosion in the anodic oxidizing atmosphere, so that the reactive $Fe^{2+}$ can be released rapidly, and $Fe^{2+}$ may not be completely consumed in a short time, and $Fe^{2+}$ at the cathode is reduced to $Fe^0$ in the reducing atmosphere at the cathode. The oxidation of NZVI is partially reversible.

### 3.3 TC removal efficiency under different voltages

Fig. 2b shows the TC removal efficiencies increased rapidly at the beginning of the reaction under 90 min. By increasing the applied voltage is able to lead to an increase in TC removal efficiency. From a thermodynamic point of view, the applied voltage must be higher than the standard potential to overcome the influencing conditions, such as concentration polarization, wire resistance and surface potential resistance.[31] The reaction preconditions of the E-NZVI system are achieved when the applied voltage is greater than 1.0 V. The higher the voltage, the faster the removal rate. This is attributed to the high reaction potential at low voltages (0.0–1.0 V) and the limited reaction kinetics limiting only NZVI adsorption and electroabsorption for TC removal. In contrast, at high voltages (2.0–4.0 V), the oxidation of NZVI is accelerated, producing a large number of reactive $Fe^{2+}$ species and $Fe^{3+}$ species with adsorption, in addition to partial electroabsorption, which accelerates the degradation of TC.[31] In contrast, at a voltage of 4.5 V, the removal efficiency of TC was 98.8%. TC removal efficiency was similar to 4.0 V (97.3%), but the removal rate was slightly higher than at 4.0 V. From the perspective of energy conservation, 4.0 V was chosen as the optimal potential for the studied electrochemical system.

### 3.4 XRD analysis

As shown in Fig. 3, the peaks at 44.5° and 82.5° of all samples can be attributed to the Fe, indicating that Fe (or Fe nuclei) is still the main component of the reacted NZVI. Compared with pristine NZVI, a new diffraction peak of $Fe_2O_3$ at 36.1° appeared in the NZVI after the non-electric reaction. The peak intensity at 44.5° was substantially weaker, while E-NZVI was similar to the original NZVI after reaction in the reaction system, and no new characteristic peaks were detected compared to the original NZVI, with only a smaller weakening of the peak intensity at 44.5°. It indicates that the NZVI can hardly be oxidized after the reaction in the E-NZVI reaction system, while the NZVI is severely oxidized after the non-electric reaction. This may be due to the reduction of $Fe^{2+}$ to $Fe^0$ by electron transfer in the electrochemical reaction system.

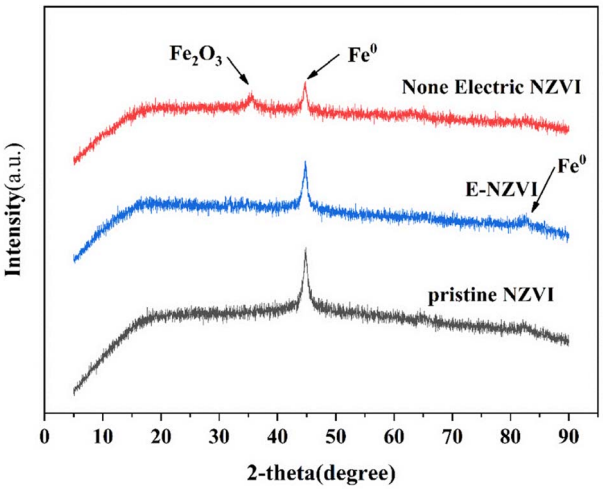


Fig. 3 XRD pattern of pristine NZVI, E-NZVI system with reacted NZVI and non-electric reacted NZVI.

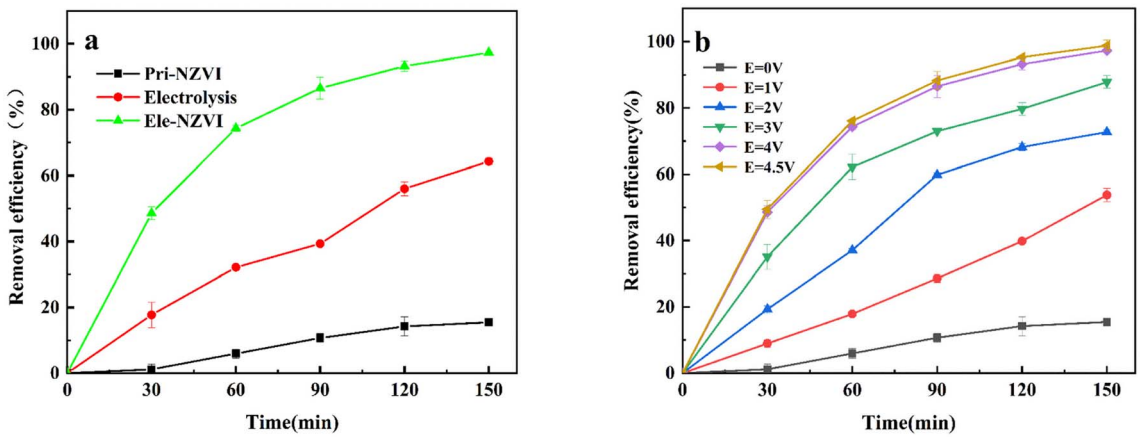


Fig. 2 (a) Removal efficiency of tetracycline under different conditions such as pristine iron, electric only and electric assisted iron; (b) removal efficiency of TC at different applied voltages (applied voltages = 4 V; $C_0$ = 30 mg $L^{-1}$; NZVI dosage = 50 mg $L^{-1}$; pH = 7.11; $t$ = 298 K); (b) removal efficiency of TC at different applied voltages ($C_0$ = 30 mg $L^{-1}$; NZVI dosage = 50 mg $L^{-1}$; pH = 7.11; $t$ = 298 K).

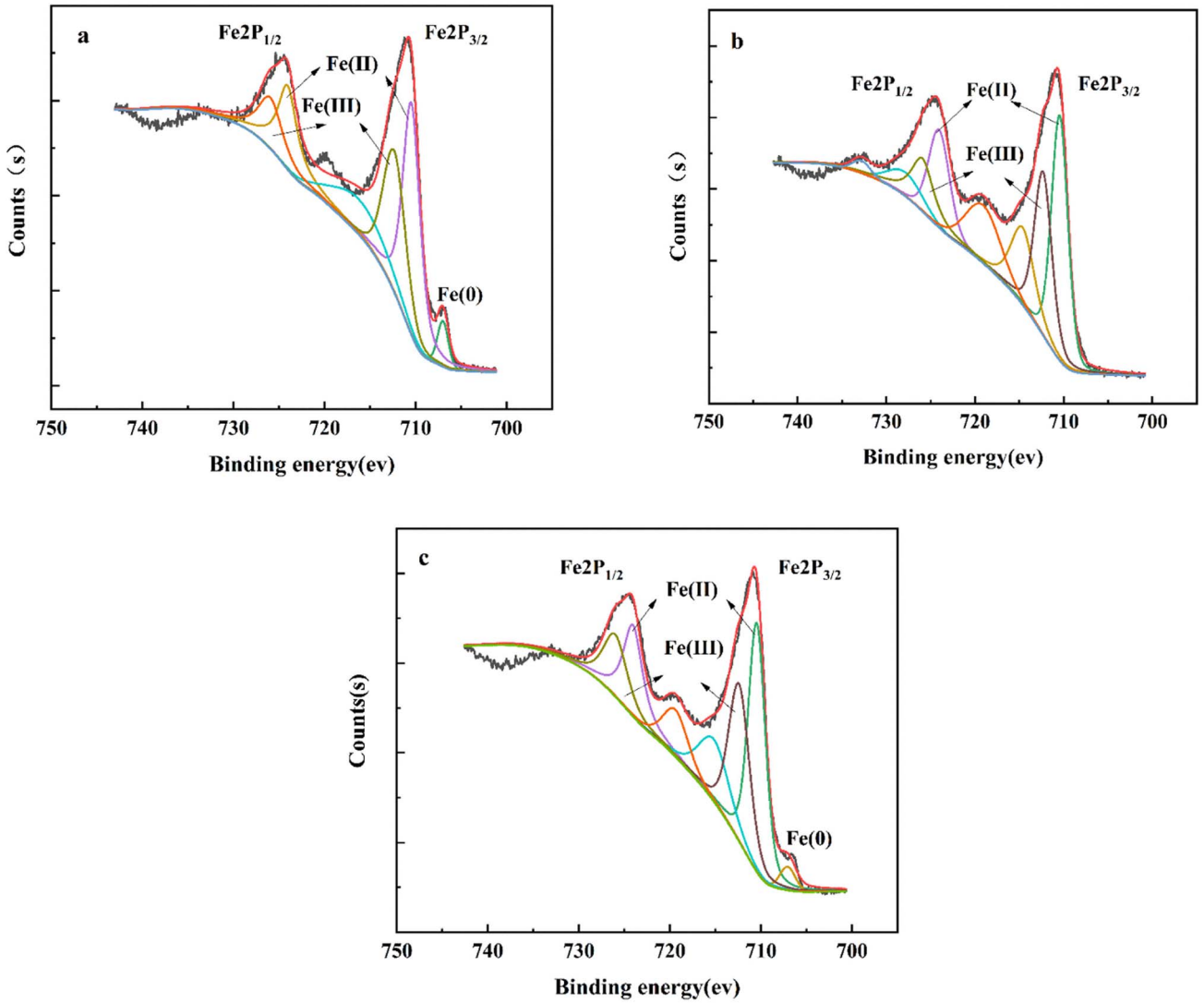


Fig. 4 High-resolution XPS spectra of Fe2p (a) NZVI raw materials and (b) NZVI after non-electric reaction, (c) NZVI after E-NZVI system reaction.

### 3.5 Analysis of XPS

Fig. 4 shows the XPS spectra of Fe2p in pristine NZVI, in E-NZVI after reaction of NZVI and in NZVI without electric reaction with TC solution in 150 min. According to the National Institute of Standards and Technology X-ray photoelectron spectroscopy database, the $2p_{3/2}$ and $2p_{1/2}$ peaks have binding energies of 711.8 eV and 725.4 eV, respectively, corresponding to the Fe(III) species. The $2p_{3/2}$ and $2p_{1/2}$ peaks at 710.8 eV and 724.3 eV, respectively, confirm the presence of the Fe(II) phase. The waste NZVI after reaction in both the pristine NZVI sample and the E-NZVI system had a similar ratio to the reacted NZVI after the reaction without charging (Fe(III) : Fe(II) = 41.38% : 58.62%, Fe(III) : Fe(II) = 43.24% : 56.76% and Fe(III) : Fe(II) = 43.09% : 56.91%), but as can be seen in Fig. 4a and c, both the original NZVI sample and the reacted NZVI from the E-NZVI system have significant $Fe^0$ peaks, demonstrating that the E-NZVI system NZVI has an antioxidant effect and the outer oxide layer produced by the accelerated corrosion of NZVI after the applied voltage could passivate the iron surface. The internal iron core is less vulnerable to oxidation.[31] In our case, the antioxidation of NZVI after the electrical addition is one of the reasons for the high TC removal efficiency of the E-NZVI system. On the contrary, although the reacted NZVI after the non-electric reaction has similar Fe(III) : Fe(II) to the original NZVI, $Fe^0$ is not present in the reacted waste NZVI. It is shown that spontaneous corrosion reactions are converting $Fe^0$ to Fe(II)/Fe(III) and converting Fe(II)/Fe(0) to Fe(III) in the non-electrified reaction system. This conclusion is consistent with the results of the XRD analysis in Section 3.4.

### 3.6 Effect of initial pH

The pH of the solution is one of the important factors affecting the removal of contaminants by zero-valent iron nanoparticles. The pH of the solution affects the electrochemical properties of zero-valent iron nanoparticles and the present form of TC by electro-assisted nano-zero-valent iron, experiments on the

removal of TC by different pH were investigated in the range of pH 2–10, with a TC concentration of 30 mg $L^{-1}$, a reaction voltage of 4 V, an electrolyte concentration of 0.1 mol per L $Na_2SO_4$, and a nano-zero-valent iron dosage of 50 mg $L^{-1}$. The effect on the removal of TC is shown in Fig. 5a the removal efficiency of TC in the E-NZVI system remained relatively stable in the initial pH range of 3.0–10.0, indicating that the initial pH was not a relative limiting factor for TC removal by electrolysis alone. This indicates that the use of electrically assisted NZVI has a wide operating pH range for TC wastewater treatment. However, it is worth highlighting that the highest removal efficiency of 100% was obtained at an initial pH of 3.0. And as the pH value increased, the removal efficiency of TC decreased. This can be explained by the fact that acidic conditions promote the corrosion of iron, which reduces the redox potential value in the solution and accelerates the reduction of TC. Lower pH may eliminate ferrous hydroxide and other protective layers accumulated on the surface of NZVI and generate more new active sites.[32] In addition, the release of $Fe^{2+}$ was promoted at lower pH conditions. However, TC removal efficiency decreased sharply to 30.05% as the pH decreased to 2. The reason for this was that the generated hydrogen would generate bubbles on the surface of NZVI (eqn (1)), which hindered the reaction of TC with NZVI. In further, the rapid corrosion of NZVI at low pH limits TC adsorption as well as Fenton/Fenton-like oxidation, thus limiting hydrogen peroxide production (eqn (2)).

$$H^+ + 2e^- \rightarrow 2[H] + H_2 \quad (1)$$

$$Fe + O_2 + 2H^+ \rightarrow H_2O_2 + Fe^{2+} \quad (2)$$

### 3.7 Effect of NZVI dosage

The effect of different NZVI dosages in E-NZVI electrolysis system on TC removal was investigated. From Fig. 5b, when the NZVI dosages were in the range of 10 mg $L^{-1}$ to 20 mg $L^{-1}$, TC removal efficiency increased less compared to that without NZVI addition. And when the dosage was increased to 30 mg $L^{-1}$, TC removal efficiency and rate increased significantly. Moreover, TC removal efficiency gradually increased as the NZVI dosage was increased from 0 mg $L^{-1}$ to 50 mg $L^{-1}$ after 150 min of reaction. And when the agent was increased to 60 mg $L^{-1}$, the removal efficiency of tetracycline was 94.8%, and the removal efficiency was slightly lower than 50 mg $L^{-1}$ (97.3%). These phenomena can be attributed to two aspects: (1)

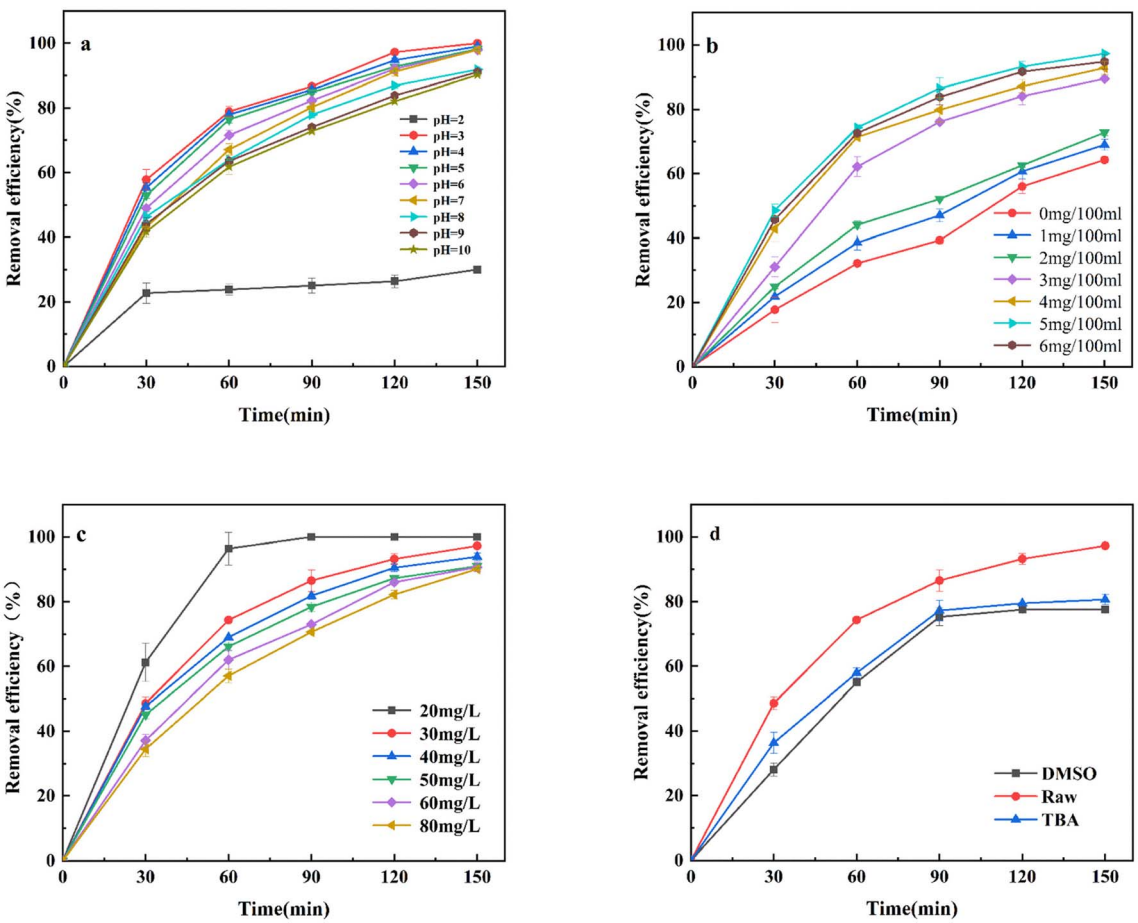


Fig. 5 Parameters affecting the degradation of TC: (a) pH value ($C_0$ = 30 mg $L^{-1}$; NZVI dosage = 50 mg $L^{-1}$; $t$ = 298 K); (b) NZVI dosage ($C_0$ = 20 mg $L^{-1}$; pH = 7.11; $t$ = 298 K) (c) initial TC concentration (NZVI dosage = 50 g $L^{-1}$; pH = 7.11; $t$ = 298 K); (d) use of quenching agents ($C_0$ = 30 mg $L^{-1}$; NZVI dosage = 50 g $L^{-1}$; pH = 7.11; $t$ = 298 K).

in the E-NZVI system, the total surface area and active sites of NZVI particles increased dramatically with the increase of the NZVI dose; (2) but when the NZVI dosage was higher than the optimal value, the reaction sites might be saturated and then their regeneration rate become a rate-limiting step. TC removal efficiency can be limited by other factors, especially the mass transfer rate of contaminants, intermediates and corrosion products between the surface of the NZVI particles and the solution.[33,34] Therefore, NZVI = 50 mg $L^{-1}$ was chosen as the optimal dosage in this study.

### 3.8 Effect of initial TC concentrations

The removal efficiency of different TC concentrations in the E-NZVI system was investigated at a voltage of 4 V, pH = 7.11. As shown in Fig. 5c, at an initial TC concentration of 20 mg $L^{-1}$, the removal efficiency was 100% for the first 90 min and then reached the degradation equilibrium. Even at the initial TC concentration of 80 mg $L^{-1}$, removal efficiency reached 90.15%. With the increase of the initial concentration of TC, TC removal did not change much. It indicates that the E-NZVI system showed excellent degradation performance for different concentration levels of TC. It can be theoretically speculated that the concentration of TC in the E-NZVI system is proportional to its concentration in the solution. The electrocatalytic activity sites of the same NZVI are similar at the same voltage intensity. Therefore, the electrocatalytic activity should be lower at lower initial TC concentrations, demonstrating that TC is mainly removed by electrochemical reactions rather than direct reduction, and the higher the initial TC concentration, the higher the energy consumption for TC reduction. In addition, the results showed that the removal efficiency of TC reached 97.95% at pH = 7, while the removal efficiency was 97.3% for the initially prepared solution pH = 7.11, so the initial pH = 7.11 of the solution was chosen as the experimental pH for saving experimental cost and obtaining high TC removal efficiency in the removal of TC.

### 3.9 Quenching experiments

Radical quenching and radical trapping experiments (with DMSO and TBA as spin-trapping agents) were employed to identify the main reactive oxygen species for TC removal by the E-NZVI system. The removal performance was inhibited to some extent in the presence of different quenching agents (Fig. 5d). The effects of several major scavengers (DMSO and TBA) on the degradation of TC by the E-NZVI system were examined to determine not only the removal efficiency under unfavorable conditions but also the role of reactive oxygen species as well as electrons in the degradation of the target pollutants. Dimethyl sulfoxide and tert-butanol scavenging compounds were added to the solution containing TC to assess the change in the efficiency of the E-NZVI system. The presence of tert-butanol ($^{\bullet}OH$ scavenger) and dimethyl sulfoxide (electron scavenger) significantly reduced the removal efficiency during E-NZVI. It is suggested that the generated $^{\bullet}OH$ is an effective reagent for the degradation of refractory organic pollutants in the electrochemical oxidation reaction, especially at the anode, where $^{\bullet}OH$ can react with organic pollutants non-selectively.[35,36] And the lone pair of electrons in the electrochemical system is also an important factor in the removal of TC.

### 3.10 Recycling experiments

To determine the recoverability of NZVI after reaction in the E-NZVI system, a recoverability test was conducted. The temperature used for this cycling test is 298 K, $C_0$ = 30 mg $L^{-1}$, NZVI dosage = 50 mg $L^{-1}$, pH is 7.11 and applied voltage is 4 V. NZVI was collected after each cycle using an extraction method. NZVI was washed three times with deoxygenated water to desorb the TC, while NZVI was later reduced with potassium borohydride in a nitrogen chamber and dried under a vacuum. Fig. 6 shows that NZVI has good recoverability after reaction in the E-NZVI system. TC removal efficiency decreased from 97.3% to 83.2% after 5 cycling steps. The above results indicate that the adsorption of NZVI on TC remained stable after the regeneration process in the E-NZVI system, and the TC could be removed efficiently and effectively during the redox process. This shows that E-NZVI has a high potential for application in TC wastewater treatment, because NZVI can be reused under the action of an applied voltage, plus it maintains a high removal efficiency after 5 consecutive cycles, making it highly cost-effective.

### 3.11 Reaction mechanism of TC removal in the E-NZVI system

**3.11.1 Reaction kinetics.** Primary or pseudo-primary reaction models are commonly used to simulate the removal of target contaminants in the base E-NZVI system. However, TC removal by E-NZVI systems is a non-homogeneous reaction that occurs on the surface of nanoparticles. Although the kinetic process can be considered to follow a pseudo-first-order model only when the NZVI reaction sites are abundant and remain constant, the two-parameter pseudo-first-order decay model takes into account not only the loss of available active sites but also the presence of inactive contaminants during the removal of contaminants from aqueous solutions.[37] Therefore, a two-

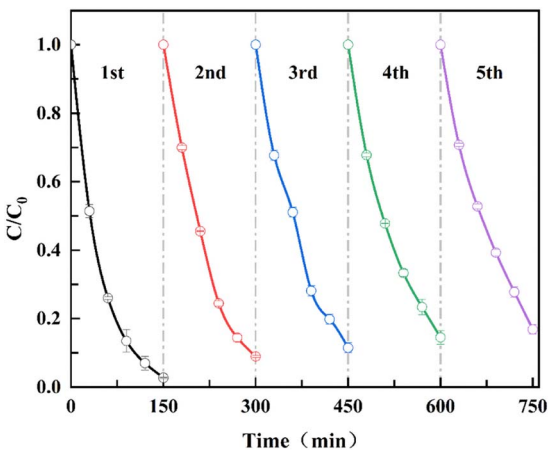


Fig. 6 Cycling of TC removal by NZVI in E-NZVI systems ($C_0$ = 30 mg $L^{-1}$; NZVI dosage = 50 mg $L^{-1}$; pH = 7.11; $t$ = 298 K).

Table 1 Fitted data for removal of TC by E-NZVI system using a two-parameter pseudo-first order decay kinetics model

| $C_0$ (mg $L^{-1}$) | Dosage (mg/100 mL) | Initial (pH) | $T$ (K) | Removal (%) | $C_{ultimate}$ (mg $L^{-1}$) | $k$ ($min^{-1}$) | $\alpha$ | $R^2$ |
|---|---|---|---|---|---|---|---|---|
| 30 | 5 | 2 | 298 | 30.05 | 20.99 | 0.05073 ± 0.01496 | 12.40451 ± 1.65137 | 0.84221 |
| 30 | 5 | 3 | 298 | 100 | 0 | 0.02628 ± 0.00128 | 0.99212 ± 0.02263 | 0.9962 |
| 30 | 5 | 4 | 298 | 99 | 0.2905 | 0.02551 ± 0.00113 | 1.00307 ± 0.02089 | 0.99681 |
| 30 | 5 | 5 | 298 | 98.2 | 0.286 | 0.0255 ± 0.00113 | 1.02611 ± 0.02135 | 0.99647 |
| 30 | 5 | 6 | 298 | 97.9 | 0.593 | 0.02224 ± 9.14639 × $10^{-4}$ | 1.00506 ± 0.01951 | 0.99705 |
| 30 | 5 | 7 | 298 | 97.95 | 0.575 | 0.02004 ± 9.77746 × $10^{-4}$ | 1.01319 ± 0.02341 | 0.99562 |
| 30 | 5 | 8 | 298 | 91.9 | 2.18 | 0.02178 ± 0.00111 | 1.00278 ± 0.02425 | 0.9954 |
| 30 | 5 | 9 | 298 | 91.1 | 2.54 | 0.01952 ± 0.00128 | 1.00575 ± 0.03135 | 0.99192 |
| 30 | 5 | 10 | 298 | 90.25 | 2.655 | 0.01989 ± 0.00103 | 0.9903 ± 0.02434 | 0.99388 |
| 20 | 5 | 7.11 | 298 | 100 | 0 | 0.03692 ± 0.0034 | 1.01387 ± 0.04312 | 0.98679 |
| 30 | 5 | 7.11 | 298 | 97.3 | 0.81 | 0.02433 ± 7.67056 × $10^{-4}$ | 0.99926 ± 0.01481 | 0.99805 |
| 40 | 5 | 7.11 | 298 | 93.95 | 2.42 | 0.02348 ± 9.21618 × $10^{-4}$ | 0.99592 ± 0.0184 | 0.99692 |
| 60 | 5 | 7.11 | 298 | 91 | 5.4 | 0.02444 ± 9.85959 × $10^{-4}$ | 1.01747 ± 0.01929 | 0.99686 |
| 80 | 5 | 7.11 | 298 | 90.7 | 5.72 | 0.02132 ± 0.00179 | 1.02865 ± 0.04073 | 0.98577 |

parameter pseudo-first-order decay model considering residual nonreactive tetracyclines was used to describe the reaction kinetics as follows:

$$C_t = C_{ultimate} + (C_0 - C_{ultimate}) \times \alpha \times \exp(-kt) \quad (3)$$

where $C_t$ (mg $L^{-1}$) is the concentration of TC in solution at reaction time $t$ (min), $C_{ultimate}$ (mg $L^{-1}$) is the concentration of unreactive TC in solution at infinite time, $C_0$ (mg $L^{-1}$) is the initial concentration of TC, $\alpha$ represents the variation coefficient for each test, and $k$ is the reaction rate constant. Clearly, a lower value of $C_{ultimate}$ implies that NZVI in the E-NZVI system has a higher reduction potential for TC, and when $C_{ultimate}$ = 0 and $\alpha$ = 1.0, eqn (3) could denote a pseudo-first-order kinetics model.

From the calculated data in Table 1, it was observed that all $\alpha$ values were close to 1.0 except for pH of 2, and the reaction of TC in the E-NZVI system could be well-described by the modified model, a two-parameter pseudo-first-order kinetics model with a correlation coefficient $R^2$ is greater than 0.9577 for all conditions except for pH of 2, which is 0.84221, indicating that the two-parameter fitted first-order decay model fits the experimental data well. The calculated values of $C_{ultimate}$ and $k$ are given in Table 1. The decrease of $C_{ultimate}$ with high $k$ indicates that TC can be effectively removed by the E-NZVI system. The value of $k$ increased with decreasing initial TC concentration, indicating that a higher initial TC concentration would restrain the removal of TC. In addition, the $k$ values and removal capacity of TC at pH 3 were the highest compared to other pH values.

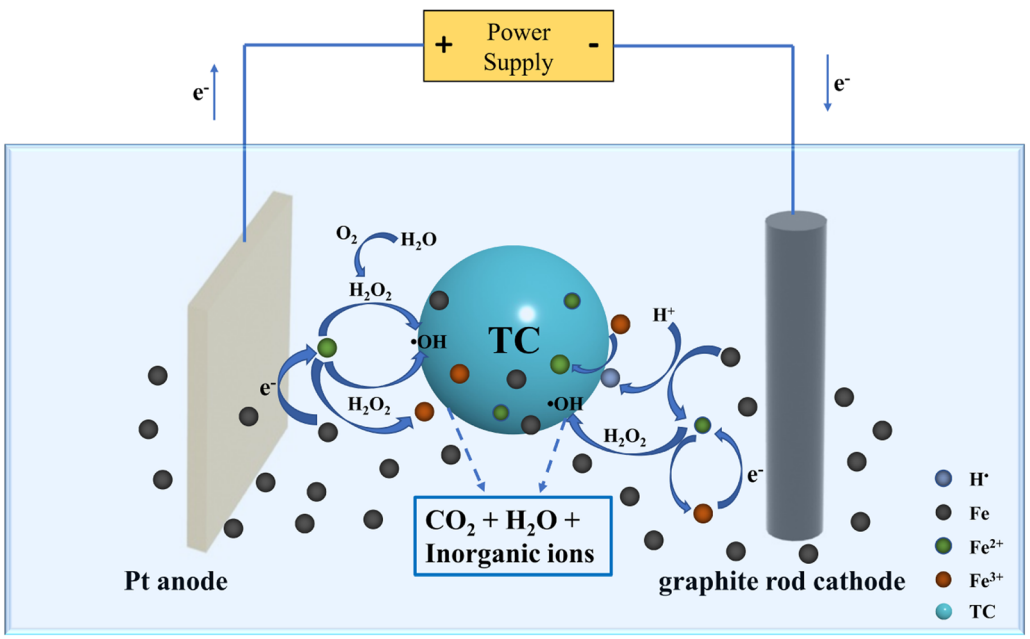


Fig. 7 Reaction mechanisms of E-NZVI process for TC treatment ($C_0$ = 30 mg $L^{-1}$; NZVI dosage = 50 mg $L^{-1}$; pH = 7.11; $t$ = 298 K).

**3.11.2 Removal mechanism of TC in E-NAVI system.** TC removal efficiency by NZVI was significantly enhanced in the presence of electrolysis under various test conditions. The reaction mechanism of the E-NZVI process is thoroughly illustrated in Fig. 7. In the presence of electrolysis, the electric field force can promote ion migration and induce convective motion in the electrolyte, which then transports $Fe^{2+}$ from the $Fe^0$ surface and $H^+$ to the $Fe^0$ surface (eqn (4)). Then, the electrons released from the NZVI core can react with $H^+$ to form $H^{\cdot}$.[38,39] This free radical can induce the indirect reduction of $Fe^{3+}$. In addition, the electric field effect significantly increases the efficiency of electron transfer from the NZVI core to the pollutant,[40] which in turn produces more reduction products. The promotion of electron transfer further accelerates the corrosion of NZVI, releasing more $Fe^{2+}$. Meanwhile, the released $Fe^{2+}$ is rapidly transferred from the surface of $Fe^0$, which promotes the reaction rate of (eqn (5)), releasing more $Fe^{2+}$ in turn. In addition, when charged reactants move forward to the surface of NZVI or charged products move away from the surface of NZVI, electric field forces can induce convection and promote mass transfer in solution. Therefore, the E-NZVI system can promote the corrosion of $Fe^0$ to release more $Fe^{2+}$ and enhance mass transfer, which can accelerate the removal of TC.

During long-term operation, corrosion products on the surface of $mFe^0$ particles are transformed to magnetite and magnet hematite in the absence of electrolysis, and passivation of the $Fe^0$ surface occurs, covering the reaction sites and thus preventing electron transfer from $Fe^0$ to the contaminant. In contrast, in the presence of electrolysis, it behaves as magnetic hematite. The $Fe^{3+}$ in hematite will be converted to $Fe^{2+}$ when it gets electrons in the case of electrolysis, which can further react with TC.

$$H^+ + e^- \rightarrow H^{\cdot} \quad (4)$$

$$Fe^0 \rightarrow Fe^{2+} + 2e^- \quad (5)$$

Meanwhile, as shown in Fig. 5d, the decrease in TC removal efficiency in the presence of TBA may be due to the oxidation of $^{\cdot}OH$. At the Pt anode, the hydrogen peroxide generated by the reaction of $H_2O$ and $O_2$ (eqn (6)) with $Fe^{2+}$ releases $^{\cdot}OH$ (eqn (7)), and the adsorbed $^{\cdot}OH$ discharged through water can oxidize TC.[41]

$$2H_2O + O_2 \rightarrow 2H_2O_2 \quad (6)$$

$$H_2O_2 + Fe^{2+} \rightarrow 2^{\cdot}OH + Fe^{3+} \quad (7)$$

# 4. Conclusion

We propose an effective technique to enhance the removal of TC from water by an electrolysis-assisted NZVI (E-NZVI) system. The batch experiments show that TC removal efficiency by E-NZVI was significantly enhanced under various conditions. Under acidic conditions, electrolysis can promote corrosion and retard passivation of NZVI, and electro-assisted NZVI has a wide operating pH range. During electrolysis, when charged reactants move toward the surface of NZVI or charged products move toward the surface of NZVI, the electric field force causes convective motion in the solution and promotes mass transport in the solution. The dosage of NZVI was increased from 3 mg/100 mL to 5 mg/100 mL, and TC removal efficiency gradually increased after 150 min of reaction. The degradation performance of TC in the E-NZVI system was excellent for different concentration levels. The results of TEM-EDS mapping, XRD and XPS analyses directly demonstrate that in the E-NZVI system. The application of electrolysis can stimulate corrosion and delay the passivation of NZVI. In addition, higher voltage facilitates the degradation of TC in the E-NZVI system but increases energy consumption. Therefore, the E-NZVI system, which can promote the corrosion of NZVI and release more $Fe^{2+}$, enhances mass transport and can accelerate the removal of TC.

# Author contributions

Xiangyu Wang: conceptualization, methodology, writing – review and editing, supervision, project administration, resources. Xiangmei Wang: conceptualization, methodology, data curation, writing – original draft. Iseult Lynch: methodology and supervision. Ma Jun: writing – review and editing.

# Conflicts of interest

There are no conflicts of interest to declare.

# Acknowledgements

This work was supported by the National Natural Science Foundation of China (NSFC, Grant No. 51968031), State Scholarship Fund of China Scholarship Council (CSC). The Engineering and Physical Sciences Research Council Impact Acceleration Accounts Developing Leaders (Grant No. 1001634), and EU H2020 projects NanoSolveIT (Grant Agreement 814572), RiskGone (Grant Agreement 814425), NanoCommons (Grant Agreement 731032) and CompSafeNano (Grant Agreement 101008099).

# References

1 F. Yu, S. Wang and H. Ma, Co-catalysis of metal sulfides accelerating $Fe^{2+}/Fe^{3+}$ cycling for the removal of tetracycline in heterogeneous electro-Fenton using an novel rolled NPC/CB cathodes, *Sep. Purif. Technol.*, 2021, **275**, 119200.

2 P. Kairigo, E. Ngumba, L. R. Sundberg, A. Gachanja and T. Tuhkanen, Occurrence of antibiotics and risk of antibiotic resistance evolution in selected Kenyan wastewaters, surface waters and sediments, *Sci. Total Environ.*, 2020, **720**, 137580.

3 U. Abubakar, H. T. Muhammad, S. A. S. Sulaiman, D. L. Ramatillah and O. Amir, Knowledge and self-confidence of antibiotic resistance, appropriate antibiotic

therapy, and antibiotic stewardship among pharmacy undergraduate students in three Asian countries, *Curr. Pharm. Teachnol. Learn.*, 2020, **12**(3), 265–273.

4 S. Yang, Y. Feng, D. Gao, X. Wang, N. Suo, Y. Yu, *et al.*, Electrocatalysis degradation of tetracycline in a three-dimensional aeration electrocatalysis reactor (3D-AER) with a flotation-tailings particle electrode (FPE): physicochemical properties, influencing factors and the degradation mechanism, *J. Hazard. Mater.*, 2021, **407**, 124361.

5 K. Rabe, L. Liu and N. A. Nahyoon, Electricity generation in fuel cell with light and without light and decomposition of tetracycline hydrochloride using g-$C_3N_4$/$Fe^0$(1%)/$TiO_2$ anode and $WO_3$ cathode, *Chemosphere*, 2020, **243**, 125425.

6 M. Liu, L. A. Hou, S. Yu, B. Xi, Y. Zhao and X. Xia, MCM-41 impregnated with A zeolite precursor: synthesis, characterization and tetracycline antibiotics removal from aqueous solution, *Chem. Eng. J.*, 2013, **223**(100), 678–687.

7 X. Wang, W. Lian, X. Sun, J. Ma and P. Ning, Immobilization of NZVI in polydopamine surface-modified biochar for adsorption and degradation of tetracycline in aqueous solution, *Front. Environ. Sci. Eng.*, 2018, **12**(4), 9.

8 N. Jian, Y. Dai, Y. Wang, F. Qi, S. Li and Y. Wu, Preparation of polydopamine nanofibers mat as a recyclable and efficient adsorbent for simultaneous adsorption of multiple tetracyclines in water, *J. Clean. Product.*, 2021, **320**, 128875.

9 X. Tang, Y. Huang, Q. He, Y. Wang, H. Zheng and Y. Hu, Adsorption of tetracycline antibiotics by nitrilotriacetic acid modified magnetic chitosan-based microspheres from aqueous solutions, *Environ. Technol. Innovat.*, 2021, **24**, 101895.

10 W. H. Tsai, T. C. Huang, H. H. Chen, J. J. Huang, M. H. Hsue, H. Y. Chuang, *et al.*, Determination of tetracyclines in surface water and milk by the magnesium hydroxide coprecipitation method, *J Chromatogr. A*, 2010, **1217**(3), 415–418.

11 S.-F. Pan, M.-P. Zhu, J. P. Chen, Z.-H. Yuan, L.-B. Zhong and Y.-M. Zheng, Separation of tetracycline from wastewater using forward osmosis process with thin film composite membrane – Implications for antibiotics recovery, *Sep. Purif. Technol.*, 2015, **153**, 76–83.

12 X.-W. Zhang, F. Wang, C.-C. Wang, P. Wang, H. Fu and C. Zhao, Photocatalysis activation of peroxodisulfate over the supported $Fe_3O_4$ catalyst derived from MIL-88A(Fe) for efficient tetracycline hydrochloride degradation, *Chem. Eng. J.*, 2021, **426**, 131927.

13 Y. Zhou, T. Cai, S. Liu, Y. Liu, H. Chen, Z. Li, *et al.*, N-doped magnetic three-dimensional carbon microspheres@$TiO_2$ with a porous architecture for enhanced degradation of tetracycline and methyl orange *via* adsorption/photocatalysis synergy, *Chem. Eng. J.*, 2021, **411**, 128615.

14 L. Cheng, T. Jiang, K. Yan, J. Gong and J. Zhang, A dual-cathode photoelectrocatalysis-electroenzymatic catalysis system by coupling $BiVO_4$ photoanode with hemin/Cu and carbon cloth cathodes for degradation of tetracycline, *Electrochim. Acta*, 2019, **298**, 561–569.

15 D. Belkheiri, F. Fourcade, F. Geneste, D. Floner, H. Aït-Amar and A. Amrane, Combined process for removal of tetracycline antibiotic – Coupling pre-treatment with a nickel-modified graphite felt electrode and a biological treatment, *Int. Biodeterior. Biodegrad.*, 2015, **103**, 147–153.

16 Y. Sun, M. Gu, S. Lyu, M. L. Brusseau, M. Li, Y. Lyu, *et al.*, Efficient removal of trichloroethene in oxidative environment by anchoring nano FeS on reduced graphene oxide supported nZVI catalyst: The role of FeS on oxidant decomposition and iron leakage, *J. Hazard. Mater.*, 2020, **392**, 122328.

17 X. Huang, N. Zhu, X. Wei, Y. Ding, Y. Ke, P. Wu, *et al.*, Mechanism insight into efficient peroxydisulfate activation by novel nano zero-valent iron anchored $yCo_3O_4$ (nZVI/$yCo_3O_4$) composites, *J. Hazard. Mater.*, 2020, **400**, 123157.

18 G. Gopal, H. Sankar, C. Natarajan and A. Mukherjee, Tetracycline removal using green synthesized bimetallic nZVI-Cu and bentonite supported green nZVI-Cu nanocomposite: a comparative study, *J. Environ. Manage.*, 2020, **254**, 109812.

19 S. Klas and D. W. Kirk, Advantages of low pH and limited oxygenation in arsenite removal from water by zero-valent iron, *J. Hazard. Mater.*, 2013, **252–253**, 77–82.

20 F. Yao, Q. Yang, J. Sun, F. Chen, Y. Zhong, H. Yin, *et al.*, Electrochemical reduction of bromate using noble metal-free nanoscale zero-valent iron immobilized activated carbon fiber electrode, *Chem. Eng. J.*, 2020, **389**, 123588.

21 L. Zhou, A. Li, F. Ma, H. Zhao, F. Deng, S. Pi, *et al.*, Combining high electron transfer efficiency and oxidation resistance in nZVI with coatings of microbial extracellular polymeric substances to enhance Sb(v) reduction and adsorption, *Chem. Eng. J.*, 2020, **395**, 125168.

22 Z. Liu, S. Dong, D. Zou, J. Ding, A. Yu, J. Zhang, *et al.*, Electrochemically mediated nitrate reduction on nanoconfined zerovalent iron: properties and mechanism, *Water Res.*, 2020, **173**, 115596.

23 J. Li, Z. Shi, B. Ma, P. Zhang, X. Jiang, Z. Xiao, *et al.*, Improving the reactivity of zerovalent iron by taking advantage of its magnetic memory: implications for arsenite removal, *Environ. Sci. Technol.*, 2015, **49**(17), 10581.

24 C. Xu, B. Zhang, L. Zhu, S. Lin, X. Sun, Z. Jiang, *et al.*, Sequestration of antimonite by zerovalent iron: using weak magnetic field effects to enhance performance and characterize reaction mechanisms, *Environ. Sci. Technol.*, 2016, **50**(3), 1483–1491.

25 Y. Sun, J. Li, T. Huang and X. Guan, The influences of iron characteristics, operating conditions and solution chemistry on contaminants removal by zero-valent iron: a review, *Water Res.*, 2016, **100**, 277–295.

26 J. Li, Z. Shi, B. Ma, P. Zhang, X. Jiang, Z. Xiao, *et al.*, Improving the reactivity of zerovalent iron by taking advantage of its magnetic memory: implications for arsenite removal, *Environ. Sci. Technol.*, 2015, **49**(17), 10581–10588.

27 Y. Sun, X. Guan, J. Wang, X. Meng, C. Xu and G. Zhou, Effect of weak magnetic field on arsenate and arsenite removal

from water by zerovalent iron: an XAFS investigation, *Environ. Sci. Technol.*, 2014, **48**(12), 6850–6858.

28 X. Zhu and J. Ni, The improvement of boron-doped diamond anode system in electrochemical degradation of p-nitrophenol by zero-valent iron, *Electrochim. Acta*, 2011, **56**(28), 10371–10377.

29 Y. Sun, X. Guan, J. Wang, X. Meng, C. Xu and G. Zhou, Effect of weak magnetic field on arsenate and arsenite removal from water by zerovalent iron: an XAFS investigation, *Environ. Sci. Technol.*, 2014, **48**(12), 6850.

30 F. Yao, Q. Yang, J. Sun, F. Chen, Y. Zhong, H. Yin, *et al.*, Electrochemical reduction of bromate using noble metal-free nanoscale zero-valent iron immobilized activated carbon fiber electrode, *Chem. Eng. J.*, 2020, **389**, 123588.

31 Z. Qi, R. Liu, T. P. Joshi, J. Peng and J. Qu, Highly efficient removal of selenite by electrolysis-assisted nano-zerovalent iron (nZVI): Implication for corrosion and reduction, *Chem. Eng. J.*, 2021, **405**, 126564.

32 L. Chen, R. Ni, T. Yuan, Y. Gao, W. Kong, P. Zhang, *et al.*, Effects of green synthesis, magnetization, and regeneration on ciprofloxacin removal by bimetallic nZVI/Cu composites and insights of degradation mechanism, *J. Hazard. Mater.*, 2020, **382**, 121008.

33 W. Yin, J. Wu, P. Li, X. Wang, N. Zhu, P. Wu, *et al.*, Experimental study of zero-valent iron induced nitrobenzene reduction in groundwater: The effects of pH, iron dosage, oxygen and common dissolved anions, *Chem. Eng. J.*, 2012, **184**, 198–204.

34 S. Huang, C. Xu, Q. Shao, Y. Wang, B. Zhang, B. Gao, *et al.*, Sulfide-modified zerovalent iron for enhanced antimonite sequestration: Characterization, performance, and reaction mechanisms, *Chem. Eng. J.*, 2018, **338**, 539–547.

35 J. Cai, M. Zhou, Y. Pan, X. Du and X. Lu, Extremely efficient electrochemical degradation of organic pollutants with co-generation of hydroxyl and sulfate radicals on Blue-$TiO_2$ nanotubes anode, *Appl. Catal., B*, 2019, **257**, 117902.

36 L. Xu, X. Ma, J. Niu, J. Chen and C. Zhou, Removal of trace naproxen from aqueous solution using a laboratory-scale reactive flow-through membrane electrode, *J. Hazard. Mater.*, 2019, **379**, 120692.

37 K. Lin, J. Ding and X. Huang, Debromination of tetrabromobisphenol a by nanoscale zerovalent iron: kinetics, influencing factors, and pathways, *Ind. Eng. Chem. Res.*, 2012, **51**(25), 8378–8385.

38 F. Xu, L. Chang, X. Duan, W. Bai, X. Sui and X. Zhao, A novel layer-by-layer CNT/$PbO_2$ anode for high-efficiency removal of PCP-Na through combining adsorption/electrosorption and electrocatalysis, *Electrochim. Acta*, 2019, **300**, 53–66.

39 X. Guan, Y. Sun, H. Qin, J. Li, I. M. Lo, D. He, *et al.*, The limitations of applying zero-valent iron technology in contaminants sequestration and the corresponding countermeasures: the development in zero-valent iron technology in the last two decades (1994–2014), *Water Res.*, 2015, **75**, 224.

40 M. Frasconi, H. Boer, A. Koivula and F. Mazzei, Electrochemical evaluation of electron transfer kinetics of high and low redox potential laccases on gold electrode surface, *Electrochim. Acta*, 2010, **56**(2), 817–827.

41 H.-Z. Zhao, Y. Sun, L.-N. Xu and J.-R. Ni, Removal of Acid Orange 7 in simulated wastewater using a three-dimensional electrode reactor: Removal mechanisms and dye degradation pathway, *Chemosphere*, 2010, **78**(1), 46–51.